Arabidopsis thaliana rapid alkalinization factor 1–mediated root growth inhibition is dependent on calmodulin-like protein 38

Received for publication, July 26, 2017, and in revised form, December 9, 2017 Published, Papers in Press, December 27, 2017, DOI 10.1074/jbc.M117.808881

Wellington F. Campos[‡1,2], Keini Dressano[‡1,3], Paulo H. O. Ceciliato[‡1,2], Juan Carlos Guerrero-Abad[‡1,2], Aparecida Leonir Silva[‡4], Celso S. Fiori[‡3], Amanda Morato do Canto[‡2], Tábata Bergonci[‡2], Lucas A. N. Claus[‡3], Marcio C. Silva-Filho[§5], and Daniel S. Moura[‡5,6]

From the [‡]Laboratório de Bioquímica de Proteínas, Departamento de Ciências Biológicas, Escola Superior de Agricultura Luiz de Queiroz, ESALQ, Universidade de São Paulo, USP, Piracicaba, SP, 13418-900 and the [§]Laboratório de Biologia Molecular de Plantas, Departamento de Genética, Escola Superior de Agricultura Luiz de Queiroz, ESALQ, Universidade de São Paulo, USP, Piracicaba, SP, 13418-900, Brazil

Edited by Joseph M. Jez

Arabidopsis thaliana **rapid alkalinization factor 1 (AtRALF1) is a small secreted peptide hormone that inhibits root growth by repressing cell expansion. Although it is known that AtRALF1 binds the plasma membrane receptor FERONIA and conveys its signals via phosphorylation, the AtRALF1 signaling pathway is largely unknown. Here, using a yeast two-hybrid system to search for AtRALF1-interacting proteins in *Arabidopsis*, we identified calmodulin-like protein 38 (CML38) as an AtRALF1-interacting partner. We also found that CML38 and AtRALF1 are both secreted proteins that physically interact in a Ca^{2+}- and pH-dependent manner. CML38-knockout mutants generated via T-DNA insertion were insensitive to AtRALF1, and simultaneous treatment with both AtRALF1 and CML38 proteins restored sensitivity in these mutants. Hybrid plants lacking CML38 and having high accumulation of the AtRALF1 peptide did not exhibit the characteristic short-root phenotype caused by *AtRALF1* overexpression. Although CML38 was essential for AtRALF1-mediated root inhibition, it appeared not to have an effect on the AtRALF1-induced alkalinization response. Moreover, acridinium-labeling of AtRALF1 indicated that the binding of AtRALF1 to intact roots is CML38-dependent. In summary, we describe a new component of the AtRALF1 response pathway. The new component is a calmodulin-like protein that binds AtRALF1, is essential for root growth inhibition, and has no role in AtRALF1 alkalinization.**

Rapid alkalinization factor (RALF)[7] is a 5-kDa peptide hormone, ubiquitous in the plant kingdom. It has been found in phytopathogenic fungi and was first isolated from tobacco leaf extracts using the alkalinization assay (1, 2). RALF increases the pH of extracellular media, and it inhibits root growth by repressing cell expansion (3–5).

The first *RALF* gene isolated from the leaves of tobacco plants was shown to encode a precursor protein that includes an N-terminal signal sequence followed by a non-conserved region and a conserved C-terminal sequence that harbors the active peptide (1). When fused to GFP, the tobacco RALF precursor was detected in the endoplasmic reticulum and later in the apoplast (6). In *Arabidopsis*, the genome includes a *RALF* gene family composed of 39 members; *RALF* genes are expressed in all tissues and developmental stages (7–10). In the root-specific isoform AtRALF1, a conserved dibasic site located upstream of the active peptide is essential for proper precursor processing. The subtilisin-like serine protease AtS1P has been identified as responsible for the processing of another isoform, AtRALF23 (11, 12).

The binding of AtRALF1 to the FERONIA receptor-like kinase has been demonstrated (4). FERONIA (FER) is a complex multitask receptor that partners with glycosylphosphatidylinositol-anchored proteins to convey defense signaling and developmental pathways (13, 14). Upon AtRALF1 binding, FER recruits a receptor-like cytoplasmic kinase (RPM1-induced protein kinase; RIPK) that is then transphosphorylated by FER (15). Using an ^{125}I-labeled AtRALF1, it was shown that ^{125}I-AtRALF1 binding was reduced by ~40% in the FER mutant *fer4*; this finding suggests the existence of other proteins that may work as receptors, as previously shown in tomato suspension culture experiments (4, 16). The tomato ^{125}I-azido-LeRALF peptide binds to two plasma membrane proteins, of 25 and 120 kDa, that may be involved in a receptor complex on the surface of tomato suspension-cultured cells (16). A similar pair of membrane proteins was observed when the iodinated LeRALF peptide was exposed to tobacco and alfalfa cells.

This work was supported in part by FAPESP and CNPq. The authors declare that they have no conflicts of interest with the contents of this article.
This article contains Table S1 and Figs. S1–S13.
[1] These authors contributed equally to this work.
[2] Supported by a fellowship from CNPq.
[3] Supported by a fellowship from FAPESP.
[4] Supported by a fellowship from CAPES.
[5] Research fellow of CNPq.
[6] To whom correspondence should be addressed. Tel.: 55-19-3429-4344 (ext. 17); E-mail: danielmoura@usp.br.
[7] The abbreviations and trivial name used are: RALF, rapid alkalinization factor 1; AtRALF, *A. thaliana* RALF; NaRALF, *N. attenuata* RALF; acriAtRALF1, AtRALF1 labeled with chemiluminescent acridinium; FER, FERONIA; RIPK, RPM1-induced protein kinase; CaM, calmodulin; CML, calmodulin-like; IQD, IQ67 domain; ITC, isothermal titration calorimetry; ER, endoplasmic reticulum; PI, propidium iodide; PCC, Pearson's correlation coefficient; BFA, brefeldin A; YFP, yellow fluorescent protein; GST, glutathione *S*-transferase; FM4-64, *N*-(3-triethylammoniumpropyl)-4-(6-(4-(diethylamino)phenyl)hexatrienyl)pyridinium dibromide.

This is an Open Access article under the CC BY license.

© 2018 by The American Society for Biochemistry and Molecular Biology, Inc. Published in the U.S.A.

Transgenic *Arabidopsis* plants overexpressing the isoform *AtRALF1*, *AtRALF23*, or *AtRALF8* have a semi-dwarf, bushier phenotype with short roots (11, 12, 17). In the native tobacco *Nicotiana attenuata*, where only one RALF isoform was found, transgenic plants in which the *NaRALF* gene was silenced exhibited long roots (18). Partial silencing or knockout of the *AtRALF1* isoform produced plants with longer roots (4, 19).

Calcium is a universal second messenger involved in the regulation of a diverse array of response pathways, including abiotic and biotic stimuli as well as development-related signals (20, 21). In the roots of *Arabidopsis* seedlings, the active AtRALF1 peptide induces a rapid and strong increase of cytoplasmic Ca^{2+} from extra- and intracellular stores (22). Calmodulins (CaMs) are Ca^{2+}-binding proteins that are highly conserved between plants and humans. CaMs perceive Ca^{2+} oscillations and serve as Ca^{2+} sensors to mediate cellular responses (23, 24). A distinctive set of proteins similar to CaMs, known as CaM-like (CML) proteins, also act as Ca^{2+} sensors in plants. The *Arabidopsis* genome has seven CaM and 50 CML genes that encode potential Ca^{2+} sensors (23, 25). Upon Ca^{2+} binding, conformational changes are induced in CaM/CMLs. These conformational changes affect interactions with a wide range of target proteins, modulating their activity (26, 27). In *Arabidopsis*, a broad range of CaM/CML targets have been identified to be involved in the regulation of abiotic stress responses, developmental and defense-related cellular responses, cell cycle control, and root development (28). Interestingly, a plant-specific IQ67 domain (IQD) family of CaM-interacting proteins were proposed to act as scaffold proteins integrating CaM/CML signaling, regulating cell function, shape, and growth (29, 30).

Although CaM proteins mediate intracellular Ca^{2+} signaling, they may also act as extracellular agents to regulate cell growth and development (31, 32). The CAM2 protein stimulated the proliferation of suspension-cultured cells; CAM2 was detected in the cell wall and in the culture medium (31). It was demonstrated that CAM2 specifically binds to sites on the plasma membrane (32). CML37, -38, and -39 are part of a discrete clade within the group IV of EF-hand–containing proteins in *Arabidopsis* (33). CML37 is an intracellular Ca^{2+} sensor involved in wound and herbivory response that mediates Ca^{2+} and jasmonate signaling (34). Calmodulin-like protein 38 (CML38) is involved in development and stress responses and more recently has been localized to ribonucleoprotein complexes induced by hypoxia (35, 36). The last member of this group, CML39, is also a Ca^{2+} sensor that works in the perception of light signals and function in the early seedling establishment (37).

Reports support the idea that RALF peptides act as signals to regulate cell expansion (1, 3, 4, 38, 39), and more than one receptor seems to be involved in this process (4, 16). However, we do not have a comprehensive understanding of the mechanisms underlying RALF recognition by cells. To identify potential interacting proteins and better understand the mechanisms of RALF recognition and signal transduction, we used a yeast two-hybrid system using AtRALF1 as bait. Herein, we show that AtRALF1 interacts with CML38. We demonstrate that both AtRALF1 and CML38 proteins are secreted and that the interaction occurs in the extracellular space in a Ca^{2+}- and pH-dependent manner. We further demonstrate that the inhibitory effect of AtRALF1 on root growth is dependent on CML38 and that *PRO35S:AtRALF1* plants in *cml38* mutant background exhibited normal growth despite the high accumulation of the AtRALF1 peptide. This finding suggests that, besides having a cytosolic role involved in stress, CML38 protein is also localized in the apoplast, functioning as an AtRALF1-interacting protein. Unexpectedly, CML38 does not seem to affect alkalinization response elicited by AtRALF1, suggesting that AtRALF1 may have an alternative signaling pathway that is independent of alkalinization.

Results

AtRALF1 physically interacts with CML38

To further our understanding of the signaling pathway involved in AtRALF1 responses, we searched for putative AtRALF1-interacting proteins using a yeast two-hybrid system. In our screening, preproAtRALF1 (locus at1g02900) was used as bait to identify putative interacting proteins from the CD4-10 cDNA library. Over 100 positive transformants were recovered, and cDNA clones were determined. One of the positive recovered plasmids harbored a 327-bp fragment of the 5′ region of the At1g76650 locus. The 109-amino acid sequence fragment encodes CML38, a development- and stress-related Ca^{2+}-binding protein (35, 36). To confirm the interaction and determine the region of preproAtRALF1 involved in the interaction, the full-length CML38 protein was fused to the yeast GAL4 activation domain, and preproAtRALF1 (120 amino acids), proAtRALF1 (Gly^{27}–Ser^{120}), and the mature AtRALF1 peptide (Ala^{72}–Ser^{120}) were fused to the DNA-binding domain. All constructs resulted in positive interactions, demonstrating that full-length CML38 interacts with AtRALF1 and that the mature peptide is sufficient for this interaction (Fig. 1*A*). Reciprocal testing of CML38 and the mature AtRALF1 peptide confirmed that the interaction is independent of the vector used, and the lack of interaction between CML38 and AtRALF34 suggests specificity (Fig. 1*B*). AtRALF34, like AtRALF1, is one of nine RALF isoforms from *Arabidopsis* that is closely related to the original RALF isolated from tobacco (10). We also evaluated the interaction of AtRALF1 with the closest CML38 homologs, CML37 and CML39. Neither CML37 nor CML39 interacted with AtRALF1 in the yeast two-hybrid assay, confirming that the interaction is specific (Fig. S1).

The interaction between CML38 and AtRALF1 was further analyzed *in vitro* using pulldown assays. Both proteins were expressed in *Escherichia coli* and purified using affinity chromatography. The AtRALF1 peptide was incubated with the GST-CML38 protein and Ca^{2+} and pulled down using glutathione immobilized on agarose (Fig. 1*C*). The addition of EGTA to the incubation buffer abolished this interaction. AtRALF1 was not pulled down when incubated only with glutathione-agarose beads. The CML38 double band observed in the presence of Ca^{2+} is probably due to a change in mobility caused by Ca^{2+} binding. Such an effect was reported for CML38 (35). The CML38/AtRALF1 physical interaction was sensitive to the pH of the interaction buffer. At a pH of 7.5, the AtRALF1 peptide

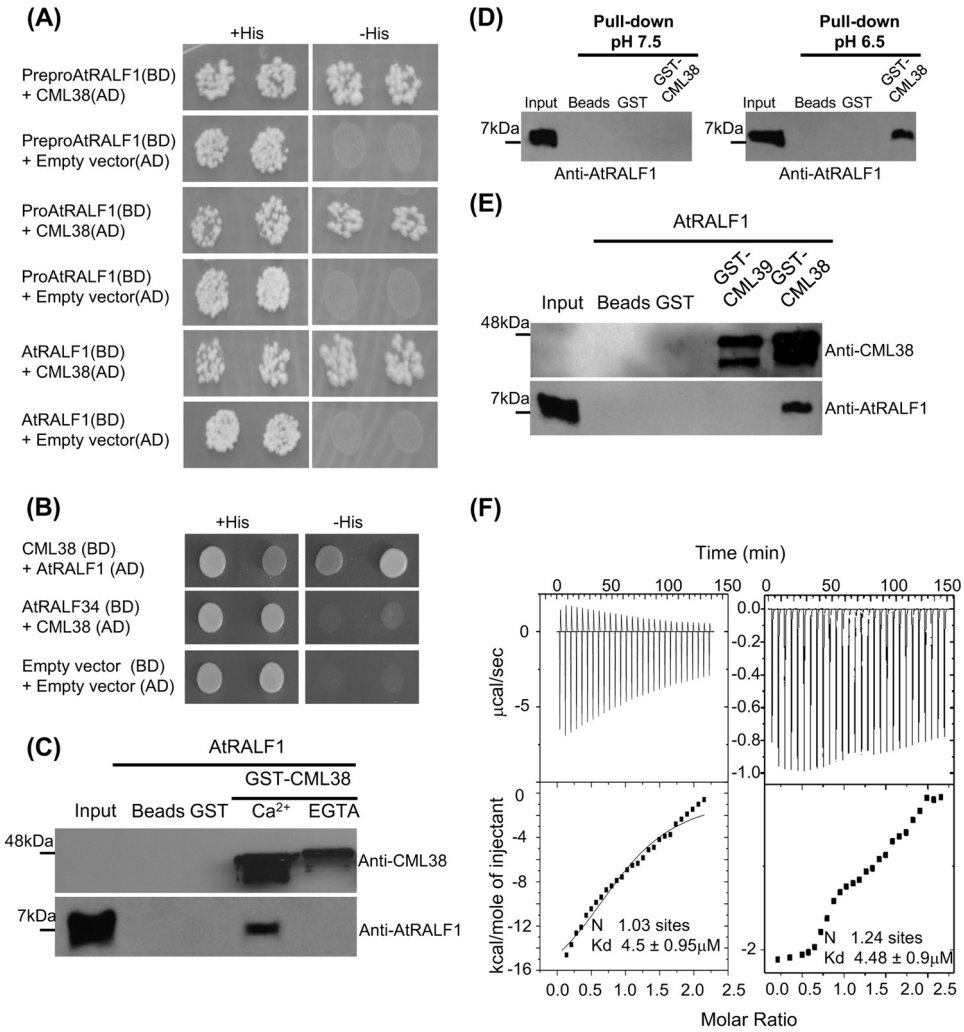

Figure 1. The AtRALF1 peptide interacts with the CML38 protein. *A* and *B*, yeast two-hybrid assay on complete (+*His*) or selective medium (−*His*). *AD*, activation domain construct; *BD*, binding domain construct. *C*, pulldown assay with the recombinant proteins AtRALF1 and GST-CML38 in the presence of Ca^{2+} or the Ca^{2+} chelator EGTA. *D*, pulldown assay with the recombinant proteins AtRALF1 and GST-CML38 in identical incubation buffers with different pH values. *E*, pulldown assay with the recombinant proteins AtRALF1, GST-CML38, and the closest homolog to CML38, GST-CML39. *F*, ITC of CML38 *versus* AtRALF1 in 15 mM HEPES, pH 6.8. ITC experiments were simulated using the following parameters. *Left*, 28 injections of AtRALF1 (0.3 mM, volume 10 µl) on CML38 (0.03 mM), cell volume = 1.4 ml at 25 °C. *Right*, 28 injections of CML38 (0.3 mM, volume 10 µl) on AtRALF1 (0.03 mM), cell volume = 1.4 ml at 25 °C. The number of sites and K_d were estimated subtracting the heats of dilution from the heats of titration (*left* and *right*) and using inversion (*right* only).

was not pulled down with GST-CML38. At a pH of 6.5, the peptide was pulled down as expected (Fig. 1*D*). The CML38 protein has 76% amino acid sequence identity with CML39 (At1g76640), the most closely related protein in the *Arabidopsis* CML family (23). To further test the specificity between CML38 and AtRALF1, we produced a GST-CML39 protein. GST-CML39 was not able to pull down the AtRALF1 peptide (Fig. 1*E*). To quantify the CML38/AtRALF1 interaction, we performed isothermal titration calorimetry (ITC) assays. In this assay, precise quantitative measurements of the heat generated/absorbed when molecules interact are taken and used to determine the equilibrium dissociation constant (K_d) and binding stoichiometry (N) of the interaction between two or more molecules in solution (40). Because AtRALF1 self-associates when in high concentrations, as indicated by the positive peaks in Fig. 1*F* (*left*) (also see Fig. S2), ITC assays were performed injecting AtRALF1 as ligand, but also reversing the titration and injecting CML38 as ligand (Fig. 1*F*, *right*). In both assays, the estimated AtRALF1/CML38 stoichiometry was ~1:1 (N = 1.03 and 1.24), and the estimated K_d was 4.5 and 4.48 µM (Fig. 1*F*). The addition of EDTA avoided the binding, and the only energy quantified by the ITC was the endothermic process produced by the AtRALF1 dilution (Fig. S2). Our results demonstrate that the CML38 protein and the AtRALF1 peptide physically interact and that the interaction is Ca^{2+}- and pH-dependent.

Both the AtRALF1 and CML38 proteins are secreted

RALF peptides have a standard secretion signal at the N terminus. To confirm that AtRALF1 is secreted, we developed a *PROAtRALF1:AtRALF1-GFP* construct and stably integrated into the *Arabidopsis* genome. The fluorescence signal from *PROAtRALF1:AtRALF1-GFP* was detected inside root cells in structures that resemble the ER (Fig. 2*A*). Fluorescence was also detected in the apoplast, as shown by colocalization with cell wall dye propidium iodide (PI) and in partially plasmolyzed root cells (Fig. 2, *B* and *C*). The colocalization between AtRALF1-GFP and PI was quantified by cross-correlation analysis (41). Both AtRALF1-GFP and PI images (Fig. 2*B*, *inset*) were ana-

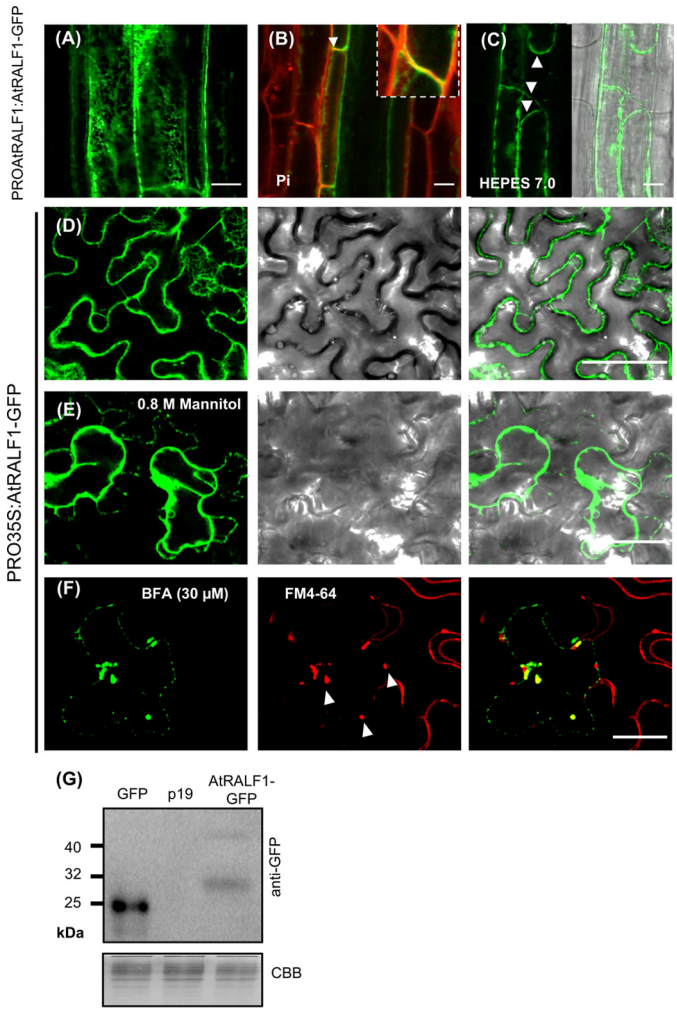

Figure 2. AtRALF1 is secreted via the default secretory pathway. *A–C* show the *AtRALF1-GFP* gene driven by its native promoter (*PROAtRALF1:ATRALF1-GFP*) expressed in the root cells of 4-day-old seedlings. The AtRALF1-GFP signal is seen in structures like the ER (*A*) and partially in the apoplast of endodermal cells (*B*); an *arrowhead* indicates the colocalization of GFP signal and the cell wall dye PI, and magnification is shown in the *inset*. Treatment with HEPES (10 mM, pH 7.0, for 4 h) was used to enhance the GFP signal in the apoplast of an endodermal cell partially plasmolyzed with 0.8 M mannitol for 30 min (*C*). A *merged image* of GFP and the bright field is shown. *Bars*, 10 μm. *Arrowheads*, plasma membrane and cell wall. *D*, *AtRALF1-GFP* gene driven by the constitutive 35S promoter (*PRO35S:AtRALF1-GFP*) in *N. benthamiana* leaf epidermal cells. The AtRALF1-GFP signal is seen in structures like the ER and at the periphery of epidermal cells. *E*, a similar set of cells showed in *D* plasmolyzed by 0.8 M mannitol. *Merged images* of GFP and the bright field are shown in *D* and *E* in the *far-right panels*. *Bars*, 50 μm. *F*, *N. benthamiana* leaf epidermal cells expressing *PRO35S:AtRALF1-GFP* treated with BFA. BFA bodies (*arrowheads*) were stained with FM4-64 (15 min). A *merged image* is shown (*far-right panel*). *Bars*, 50 μm. *G*, protein blot of extracts from *N. benthamiana* leaves expressing *PRO35S:GFP*, p19, and *PRO35S:AtRALF1-GFP* probed with anti-GFP antibody. *CBB*, Coomassie Brilliant Blue.

lyzed by computationally shifting the image, and Pearson's correlation coefficient (PCC) was calculated. Analysis of merged AtRALF1-GFP and PI images showed an average PCC value of 0.52 ± 0.07, supporting the colocalization of the AtRALF1-GFP and PI. Using the promoter 35S, we transiently expressed the construct *PRO35S:AtRALF1-GFP* into *Nicotiana benthamiana* leaves. The GFP fluorescent signal was localized at the periphery of cells, and when cells were plasmolyzed by mannitol (0.8 M), the fluorescent signal was localized in the apoplast and cytoplasm (Fig. 2, *D* and *E*). Cells expressing *PRO35S:AtRALF1-GFP* further treated with brefeldin A (BFA), an inhibitor of protein secretion via ER-Golgi that causes the formation of endosomal aggregates (BFA bodies/compartments), showed a reduction in the GFP fluorescence at the periphery of cells and the presence of the small aggregates resembling BFA bodies/compartments (Fig. 2*F*). FM4-64 (*N*-(3-triethylammoniumpropyl)-4-(6-(4-(diethylamino)phenyl)hexatrienyl)pyridinium dibromide) is a lipophilic dye that labels cell membranes and stains intracellular BFA bodies/compartments (42). Colocalization of AtRALF1-GFP aggregates with FM4-64-stained BFA-induced bodies in cells transiently expressing *PRO35S:AtRALF1-GFP* (average PCC = 0.77 ± 0.1) indicates that AtRALF1-GFP protein is secreted via a default secretory pathway. Confirmation of AtRALF1 secretion via the default pathway was also demonstrated using colocalization with an ER marker (Fig. S3). Protein extracts from leaves transiently expressing AtRALF1-GFP showed an anti-GFP antibody–reactive band of ~30 kDa corresponding to AtRALF1-GFP chimeric protein (Fig. 2*G*).

CML38 does not have a typical secretion signal, and when the protein was fused to 3 copies of the yellow fluorescent protein (YFP), the CML38-YFP-YFP-YFP was found in ribonucleoprotein complexes (36). However, SecretomeP, a sequence-based neural-network method for predicting leaderless protein secretion, gives CML38 a neural-network score of 0.808, well above the 0.5 minimum considered to predict extracellular localization (43). Because AtRALF1 physically interacts with CML38 and there is no evidence that AtRALF1 peptide is cytosolic, we further investigated the subcellular localization of CML38. Although several attempts were made using the chimeric gene *PROCML38:CML38-GFP*, we were unable to detect a fluorescence signal in untreated transgenic plants harboring the construct. However, with the 35S promoter, we transiently introduced the construct *PRO35S:CML38-GFP* into *N. benthamiana* leaves, and the GFP fluorescent signal was localized at the periphery of cells (Fig. 3*A*). To distinguish between the GFP signal in the apoplast and in the cytoplasm, epidermal cells were also plasmolyzed. Partially plasmolyzed cells showed a CML38-GFP fluorescent signal in the apoplast and cytoplasm (Fig. 3*B*). Even without a typical signal sequence, the localization of the chimeric CML38-GFP protein suggests that CML38 is secreted. To investigate whether CML38 secretion occurs via the default secretory pathway, we incubated *N. benthamiana* leaves expressing the *PRO35S:CML38-GFP* gene with BFA and the dye FM4-64. As opposed to what was observed for AtRALF1-GFP, neither reduction in CML38-GFP signal nor colocalization with FM4-64-stained BFA-induced bodies was found (Fig. 3*C*). Undetectable CML38-GFP signal in *PROCML38:CML38-GFP* plants is probably due to low gene expression conferred by its own promoter. Because *CML38* gene expression is induced by AtRALF1 and hypoxia (Fig. S4) (36), we used both treatments to induce the CML38-GFP transgene in the root cells of *PROCML38:CML38-GFP* plants. *PROCML38:CML38-GFP* plants treated with 1 μM AtRALF1 peptide showed GFP fluorescence signal at the periphery of root cells (Fig. 3*D*). Root cells expressing CML38-GFP were stained with cell wall dye PI, and the overlay of images from the two detection channels was used to calculate the PCC of the two fluorescent signals. An average PCC value of 0.19 ± 0.06

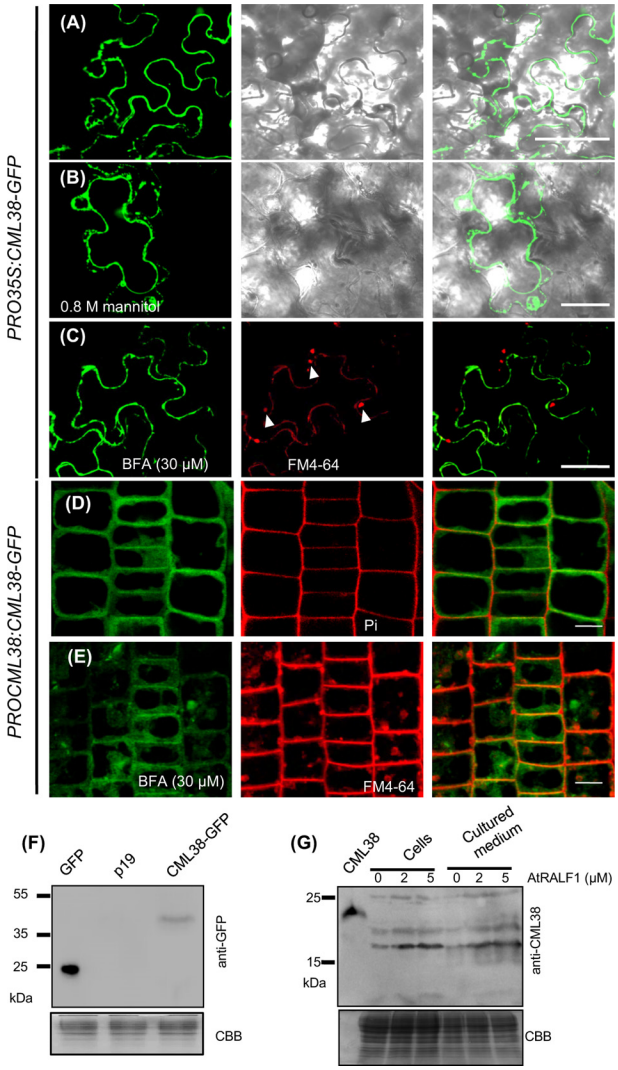

Figure 3. CML38 is secreted via an unconventional protein secretion pathway. *A*, *CML38-GFP* gene driven by the constitutive 35S promoter (*PRO35S:CML38-GFP*) in *N. benthamiana* leaf epidermal cells. The CML38-GFP signal is seen at the periphery of epidermal cells. *B*, a set of cells similar to that shown in *A* plasmolyzed by 0.8 M mannitol. *Merged images* of GFP and the bright field are shown in *A* and *B* in the *far-right panels*. *Bars*, 50 μm. *C*, *N. benthamiana* leaf epidermal cells expressing *PRO35S:CML38-GFP* treated with BFA. BFA bodies (*arrowheads*) were stained with FM4-64 (15 min). A *merged image* is shown (*far-right panel*). *Bars*, 50 μm. *D*, *CML38-GFP* gene driven by its native promoter (*PROCML38:CML38-GFP*) in root cells (4 days old) treated with AtRALF1 (1 μM, 4 h). Roots were stained with PI. *E*, roots of *PROCML38:CML38-GFP* seedlings induced by AtRALF1 and incubated with BFA (30 min). BFA bodies were stained with FM4-64 (15 min). *Bars*, 10 μm. *Merged images* are shown in the *far-right panels*. *F*, protein blot of extracts from *N. benthamiana* leaves expressing *p35S:GFP*, p19, and *p35S:AtRALF1-GFP* probed with anti-GFP antibody. *CBB*, Coomassie Brilliant Blue. *G*, protein blot of extracts from *Arabidopsis* cells (*MM1*) and cultured medium of suspension cells induced by AtRALF1 (2 and 5 μM, 4 h). Blots were probed with anti-CML38 antibody. *CML38*, recombinant CML38 protein with a His tag (21.73 kDa).

was obtained, indicating an existing although low correlation between both signals. Although *CML38* gene induction by hypoxia was also observed, the increase in fluorescence signal appears lower than when induced by AtRALF1 treatment (Fig. S5). We next evaluated the FM4-64–stained root cells of CML38-GFP–expressing plants treated with AtRALF1 and BFA. FM4-64–stained aggregates did not colocalize with CML38-GFP signal (Fig. 3*E*, average PCC = 0.08 ± 0.03). The integrity of the CML38-GFP fusion protein was confirmed by protein blotting (Fig. 3*F*). Immunodetection of the native CML38 protein in extracts from cells and culture medium of *Arabidopsis* cell suspensions with or without AtRALF1 treatment was also performed. An anti-CML38 antibody–reactive band of ~20 kDa corresponding to CML38 protein was detected in cell and culture medium extracts, and in both extracts, the amount of accumulated protein was increased by AtRALF1 treatment (Fig. 3*G*). The subcellular localization of the AtRALF1-GFP and CML38-GFP fusion proteins demonstrates that although both proteins are found in the apoplast, the former is secreted via the default secretory pathway and the latter is secreted unconventionally.

CML38 T-DNA insertion mutants are insensitive to AtRALF1

To examine whether AtRALF1 response is dependent on the presence of CML38, we obtained two T-DNA insertion mutants defective in *CML38* gene expression (*cml38-1* and *-2*). We used wildtype plants and a *CML39* T-DNA insertion mutant (*cml39*) as controls. All mutants were confirmed to be knockout lines homozygous for T-DNA insertions (Fig. S6). Mutant seedlings (2 days old) were incubated for 48 h in liquid media with or without 5 μM of AtRALF1, and their root growth was evaluated. Wildtype and *cml39* mutant seedlings were inhibited by the AtRALF1 peptide; the same treatment had no effect on *cml38-1* and *cml38-2* seedlings (Fig. 4*A*). In another experiment, *cml38-1* and *-2* plants were evaluated later, and similar results were observed (Fig. 4*B*). A side-by-side experiment with CML38 mutants and *fer4* showed that the insensitivity of the CML38 mutants is not dose-dependent (Fig. S7). FERONIA knockout plants show longer primary root than wildtype plants only when under blue light (4). CML38 mutants show longer primary root than wildtype plants under white light. Under blue light treatment, the root length of *cml38* mutants is even larger (Fig. 4*B* and Fig. S8). Our results suggest that AtRALF1 and CML38 are both secreted proteins. Therefore, we examined whether exogenous CML38 protein could rescue the AtRALF1 sensitivity phenotype in *cml38* mutants. The addition of CML38 protein to medium containing the AtRALF1 restored the root inhibitory activity of the peptide in the *cml38-1* and *-2* mutants, whereas the addition of CML39 to media containing the AtRALF1 did not restore (Fig. 4*C*). The application of only CML38 or CML39 to either wildtype or *cml38* seedlings had no effect on root growth. We also crossed the *PROCML38:CML38-GFP* plant with the *cml38-1* mutant to re-introduce the *CML38* gene into the mutant background. Plants from the F3 generation, selected for the presence of the *PROCML38:CML38-GFP* gene and absence of the endogenous CML38, were exposed to the AtRALF1 peptide and showed restoration of the AtRALF1 sensitivity phenotype (Fig. 4*D* and Fig. S9*A*). Root growth assays demonstrated that both *cml38* mutants are insensitive to the inhibitory effect of the AtRALF1 peptide. These findings suggest that the CML38 protein is an absolute requirement for the root growth inhibition caused by AtRALF1. We examined the effect of an anti-CML38 antibody on the AtRALF1 root growth inhibition. Our rationale was that the antibody would sequester the available CML38 in the apoplast. The exogenous treatment with only anti-CML38 antibody caused the roots to grow longer (Fig. 4*E*). This effect could

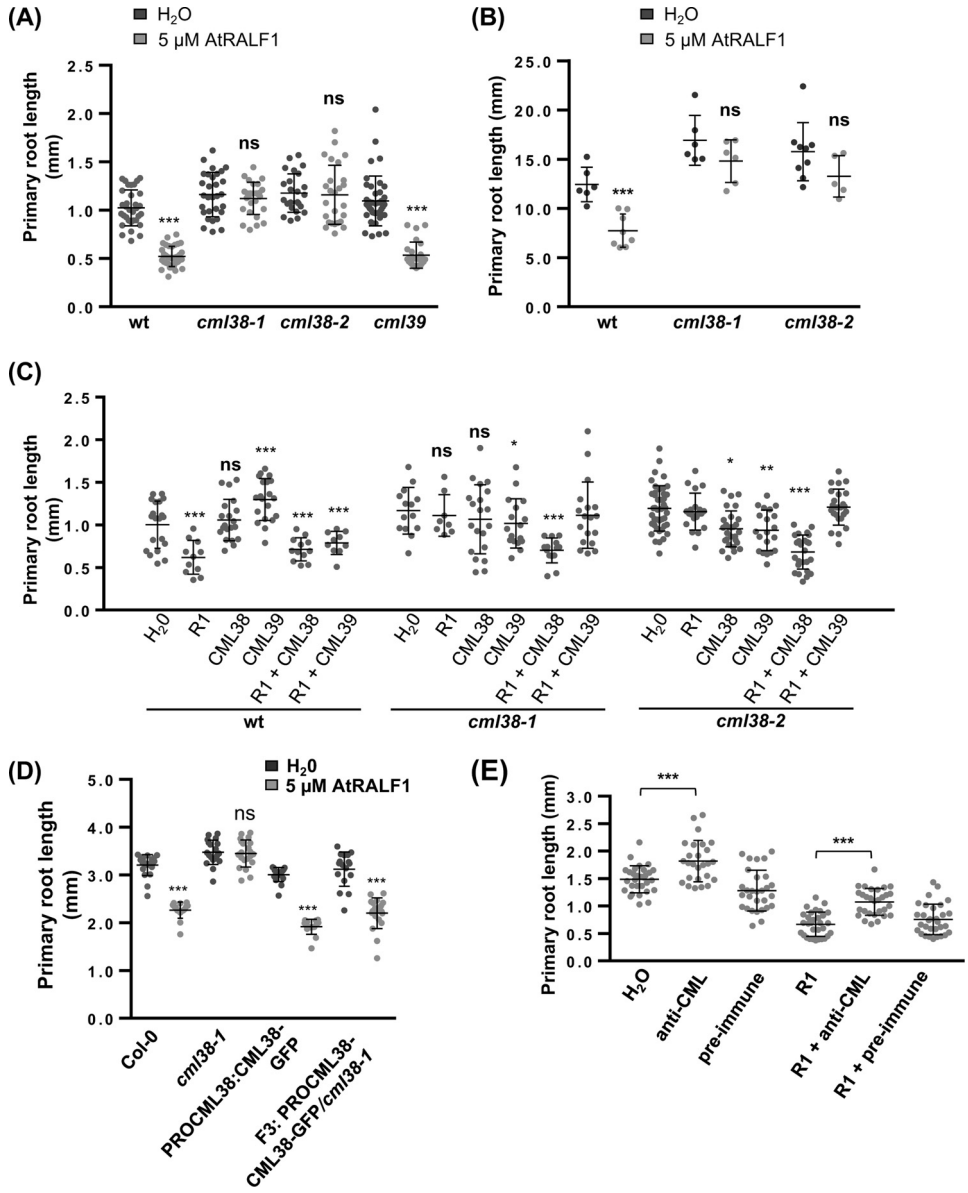

Figure 4. *cml38* mutants are insensitive to the inhibitory activity of AtRALF1 on root growth, and sensitivity is restored by exogenous treatment with CML38 or by introgression of the *PROCML38:CML38-GFP* gene. *A*, *Arabidopsis* seedlings (2 days old) were treated with AtRALF1 for 48 h. Values are the means ± S.D. (*error bars*) of at least 25 seedlings. ***, $p < 0.001$ (Student's *t* test). *ns*, not significant. *B*, 2-day-old seedlings were transferred to medium containing 5 μM of AtRALF1, and the root length was measured after 6 days of treatment. Data represent mean values ± S.D. ($n = 15$). Student's *t* tests were used to compare treated with AtRALF1 and water control. ***, $p < 0.001$. *C*, *Arabidopsis* seedlings (2 days old) were treated with AtRALF1 (*R1*), CML38, or CML39 proteins for 48 h. Values are means ± S.D. (*error bars*) of 35 seedlings. *, $p < 0.05$; **, $p < 0.01$; ***, $p < 0.001$ (Student's *t* test). *D*, introgression of the *PROCML38:CML38-GFP* gene into the *cml38-1* mutant restores the root growth inhibition caused by AtRALF1. Two-day-old parental lines *cml38-1* and *PROCML38:CML38-GFP* or F3 progeny *PROCML38:CML38-GFP/cml38-1* were treated with water or AtRALF1 for 3 days. Values are the means ± S.D. of at least 30 seedlings. ***, $p < 0.01$ (Student's *t* test). *E*, *Arabidopsis* seedlings (2 days old) were treated with water, AtRALF1 (R1), 12 μg of anti-CML38 (anti-CML) antibody, 12 μg of preimmune serum, or combinations of the peptide with anti-CML or preimmune serum for 48 h. Values are means ± S.D. of 30 seedlings. ***, $p < 0.001$ (Student's *t* test).

be explained by sequestration of endogenous CML38 leading to derepression of cell expansion or a still unidentified RALF-independent action of CML38. Simultaneous treatment with both AtRALF1 and anti-CML38 antibody also induced the roots to grow longer than the seedlings that were treated with AtRALF1 only; treatment with preimmune serum or preimmune serum in combination with AtRALF1 did not produce this effect (Fig. 4*E*). A set of AtRALF1-inducible genes has been reported (19). We tested whether the presence of *CML38* is a requirement for the induction of AtRALF1-inducible genes. None of the genes tested were induced in the *cml38-1* and *cml38-2* T-DNA insertion mutants (Fig. S9*B*). Although the lack of *CML38* causes the insensitivity to AtRALF1, the overexpression of the *CML38* gene did not show hypersensitivity (Fig. S10). None of the 17 *PRO35S:CML38* lines obtained exhibited an abnormal phenotype. Altogether, these results indicate that CML38 is essential for AtRALF1 recognition. However, the presence of CML38 is not a rate-determining step. RALF peptides induce the rapid and strong alkalinization of the extracellular media of cell suspension cultures (1). Unexpectedly and in contrast to root inhibitory activity, alkalinization assays demonstrate that CML38 does not cause alterations in the pH of the extracellular

media, indicating that CML38 is not essential for the alkalinization response (Fig. S11, *A* and *B*). Both *cml38* mutants treated with AtRALF1 showed normal alkalinization of the rhizosphere in media containing the pH indicator bromcresol purple and no hypersensitivity to lithium ions as opposed to *fer4* mutants (Fig. S11, *C–E*). Altogether, our results suggest that CML38 is not involved in the alkalinization response caused by AtRALF1.

CML38 is essential for the semi-dwarf phenotype produced by AtRALF1 overexpression

Arabidopsis plants transformed with the *AtRALF1* gene under the control of the 35S promoter (*PRO35S:AtRALF1*) exhibit reduced root growth and a semi-dwarf phenotype (11). To determine whether CML38 is essential for this phenotype *in planta*, we introduced the *PRO35S:AtRALF1* construct into the *cml38* background by crossing both *PRO35S:AtRALF1* semi-dwarf plants with the *cml38-1* mutant. Lines homozygous for the *PRO35S:AtRALF1* transgene and the T-DNA insertion were selected from 70 F2 descendants from a *cml38–1* × *PRO35S:AtRALF1* cross. The evaluated *cml38-1/PRO35S:AtRALF1* line had no detectable *CML38* expression, and the levels of *AtRALF1* mRNA were similar to the levels found in the parent line *PRO35S:AtRALF1* (Fig. 5*A*). To ensure that the peptide accumulated as in the original parent line *PRO35S:AtRALF1*, we isolated the active AtRALF1 peptide (11). In plants overexpressing AtRALF1 in *cm38-1* mutant background (*cml38-1/PRO35S:AtRALF1*), the peptide accumulated similarly to the *PRO35S:AtRALF1* parent line (Fig. 5*B*). Homozygous plants descending from the *cml38-1/PRO35S:AtRALF1* plants were grown on vertical plates, and their root length was evaluated (Fig. 5*C*). The root length of *cml38-1/PRO35S:AtRALF1* plants was similar to that of the *cml38-1* mutant. The root length of both plants overexpressing AtRALF1 in cml38-1 mutant background and mutant was longer than that in the wildtype plants used as the control. Hypocotyl elongation of dark-grown *PRO35S:AtRALF1* seedlings was also reduced compared with wildtype (19). The hypocotyl length of *cml38-1/PRO35S:AtRALF1* seedlings grown in the dark was similar to that of wildtype (Fig. 5*D*). Representative images of seedlings at the time they were measured are shown in Fig. 5 (*C* and *D*, *right panels*). The semi-dwarf phenotype observed in *cml38/PRO35S:AtRALF1* plants due to the overexpression of *AtRALF1* is dependent on the presence and expression of *CML38*.

AtRALF1 labeled with chemiluminescent acridinium (acriAtRALF1) shows decreased specific binding in cml38 mutants

Acridinium can be used as a sensitive tool for protein detection, and acridinium-labeled peptides have been used to efficiently detect specific peptide-binding sites in plant cells (44). We have produced and purified an acriAtRALF1 peptide to investigate the role of CML38 in AtRALF1 binding (Fig. S12*A*). AcriAtRALF1 showed activity similar to that of unlabeled AtRALF1 in an aequorin/Ca^{2+} assay (Fig. S12*B*). Wildtype seedlings were incubated with acriAtRALF1 and extensively washed. The acriAtRALF1 bound to seedlings was measured by exposing the seedlings to hydrogen peroxide in front of a chemiluminescence detector. In wildtype seedlings, total

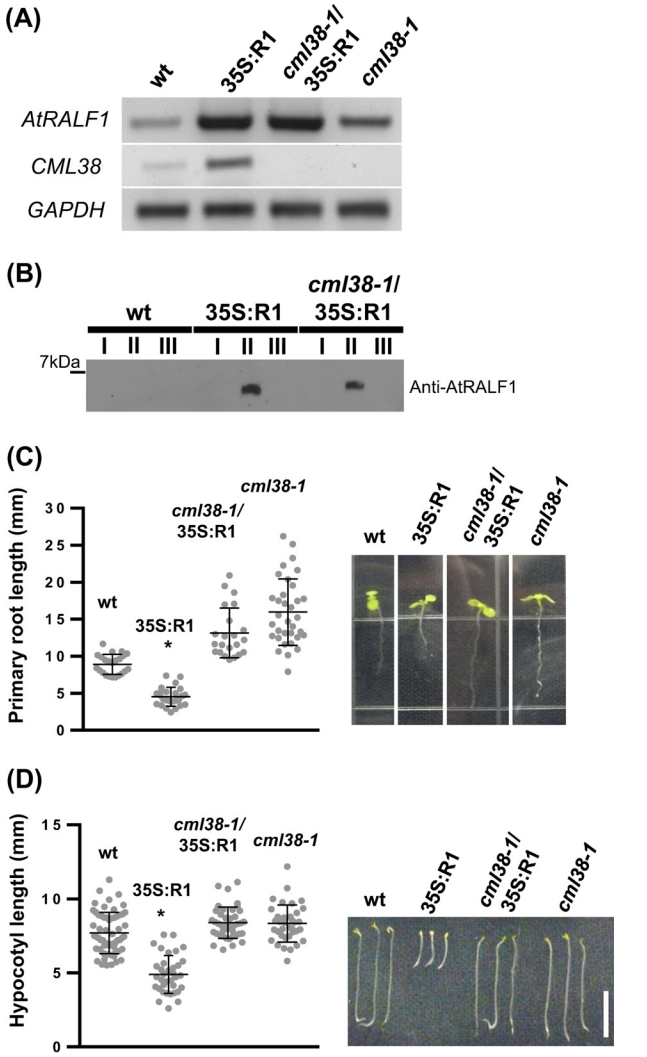

Figure 5. Gene expression analysis, AtRALF1 peptide accumulation, and phenotype of plants overexpressing the *AtRALF1* gene in the *cml38-1* mutant background. *A*, expression analysis of the *AtRALF1* and *CML38* genes in roots of 15-day-old plants. *GAPDH* expression was used as an internal control. *B*, blot of protein extracts from *Arabidopsis* seedlings. Extracts were separated by reversed-phase chromatography. *I*, *II*, and *III*, HPLC fractions. *C*, *Arabidopsis* seedlings were grown for 3 days in vertical plates for root growth measurements. Values are the means ± S.D. (*error bars*) of 34 plants. Representative images of the seedlings are shown. *D*, *Arabidopsis* seedlings were grown in the dark for 2 days for hypocotyl length measurements. *Bar*, 5 mm. Values are the means ± S.D. of at least 35 seedlings. *, significant difference ($p < 0.05$, Student's *t* test). Representative images of the seedlings are shown. *wt*, wildtype. *35S:R1*, plants overexpressing *AtRALF1*. *cml38-1/35S:R1*, plants overexpressing AtRALF1 in *cml38-1* mutant background. *cml38-1*, T-DNA insertion mutant.

acriAtRALF1 binding was reduced to 69% when a 10-fold excess of unlabeled AtRALF1 was added (Fig. 6). No reduction was observed when a 10-fold excess of AtRALF34 or AtRALF1(9–49), an inactive analog (Fig. S13), was added. A 100- or 500-fold excess of AtRALF1 further reduced acriAtRALF1 binding to 36%, demonstrating that AtRALF1-specific binding was responsible for 64% of total binding. Although the entire seedling was incubated with acriAtRALF1, the chemiluminescent signal was emitted from the roots and not from other parts of the seedling (Fig. S12*C*). When *cml38-1* and *cml38-2* mutants were incubated with acriAtRALF1, total binding was reduced to 47 and 46% of that observed in wildtype seedlings.

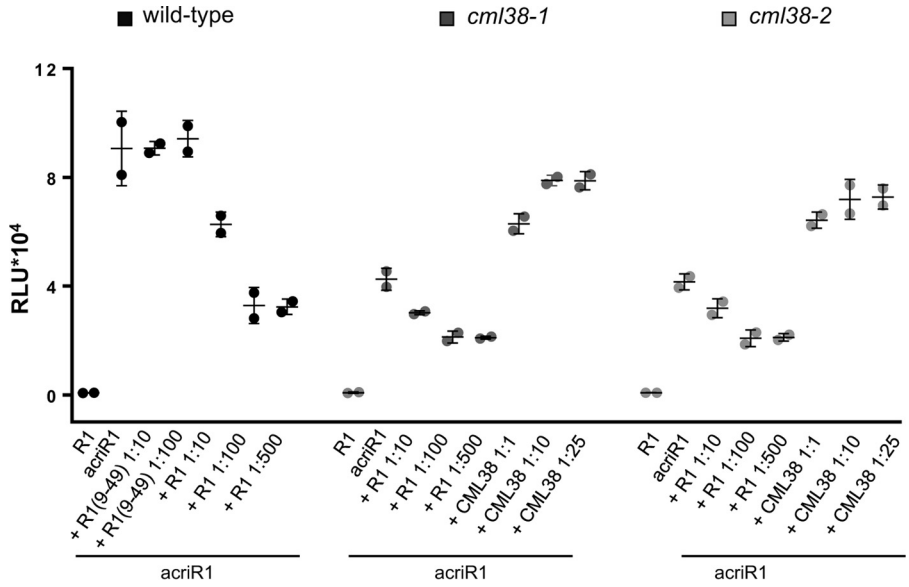

Figure 6. cml38 mutants show a reduced AtRALF1 binding to intact seedlings. Seedlings were treated for 15 min with 7 nM acriAtRALF1 (*acriR1*), acriAtRALF1 and an excess of unlabeled AtRALF1 (*R1*), RALF1(9–49) (*R1*(*R9–49*)), or CML38, as indicated. Values are the means ± S.D. (*error bars*) of two measurements (5 seedlings each). *RLU*, relative light units.

Incubation with a 10- and 100-fold excess of unlabeled AtRALF1 reduced binding to ~34 and 23% of the total, respectively. Incubation with a 500-fold excess of unlabeled AtRALF1 did not further reduce acriAtRALF1 binding. Based on the acriAtRALF1 binding observed in intact seedlings, the CML38 protein accounts for ~50% of AtRALF1 binding. Incubation of *cml38* mutants with acriAtRALF1 in the presence of a 1:1 molar ratio or 10-fold excess of CML38 protein recovered an average of 70 and 84% of the total binding observed in wildtype seedlings, respectively. The use of a 25-fold excess of CML38 protein did not further increase acriAtRALF1 binding. The addition of either CML38 or CML39 proteins to wildtype seedlings incubated with acriAtRALF1 showed no effect on total acriAtRALF1 binding; the CML39 protein was not able to recover acriAtRALF1 binding in the *cml38-1* mutant (Fig. S12*D*). Our data with acriAtRALF1 demonstrate that the binding of the peptide in intact seedlings is specific and partially dependent on CML38.

Discussion

RALF is a secreted peptide that represses cell elongation (1, 3, 4, 19, 38). During our search for proteins that interact with AtRALF1, we isolated a cDNA that encodes CML38 by using a yeast two-hybrid system. CML38 belongs to a 50-member family unique to plants. This family is composed of proteins with EF-hands that have 16–75% amino acid identity with CaMs, such as CAM2 (25, 45). Few CMLs have been characterized, and their functions in plants are still largely unknown. Herein, we demonstrate that CML38 physically interacts with the peptide hormone AtRALF1 (Fig. 1). CML38 has been characterized previously as a Ca^{2+}-binding protein with a role in development and stress responses (35). AtRALF1 and CML38 are both secreted proteins. Although CML38 does not contain a typical N-terminal secretion signal, we have shown that it is secreted unconventionally (Fig. 3). Based on the subcellular localization of both AtRALF1 and CML38, the interaction occurs in the apoplast. This interaction is dependent on an acidic pH, in agreement with the acidic nature of the apoplast (46, 47). A pH-dependent interaction was also reported for CML18 (At3g03000), a vacuolar CML that interacts with a tonoplastic Na^+/H^+ antiporter (48). CaMs are well-known intracellular Ca^{2+} sensor proteins. Extracellular CaMs have also been identified and characterized to some extent in oat (49) and in cell suspensions from *Angelica dahurica*, carrot, tobacco, and *Arabidopsis* (31, 50, 51). In *Arabidopsis*, CaM is proposed to play a role as a polypeptide signal; CaM receptor-like binding proteins have been found on the cell surface (31, 32).

Initially, the following two major biological activities were attributed to RALF peptides: the inhibition of primary root growth and the alkalinization of the extracellular medium of cell suspension cultures (1). The inhibition of primary root growth was later confirmed to be a consequence of the inhibition of cell expansion (3, 4, 11, 19). We tested two *cml38* mutants in root growth assays. These mutants were insensitive to treatment with the peptide. We were also able to reestablish sensitivity upon the exogenous application of the CML38 protein (Fig. 4*C*). Although the role of extracellular CaMs in plant growth has been investigated for quite some time, it remains enigmatic. The exogenous application of CaM proteins from *Arabidopsis* and cauliflower has been shown to enhance the division of suspension culture cells and the growth of pollen tubes, respectively (31, 52). However, only high concentrations of CaM inhibitors are able to inhibit root growth. Concentrations of CaM antagonists as high as 1 μM have been shown to have no effect on root growth (53, 54). Based on our data, it is unlikely that CML38 has a positive effect on growth. If CML38 enhances growth, the role of AtRALF1 would be its sequestration in the apoplast and the consequent inhibition of its enhancer effect. In that case, *cml38* mutants would have short roots due to the lack of the enhancer CML38, an effect also expected when wildtype seedlings would be exposed to anti-

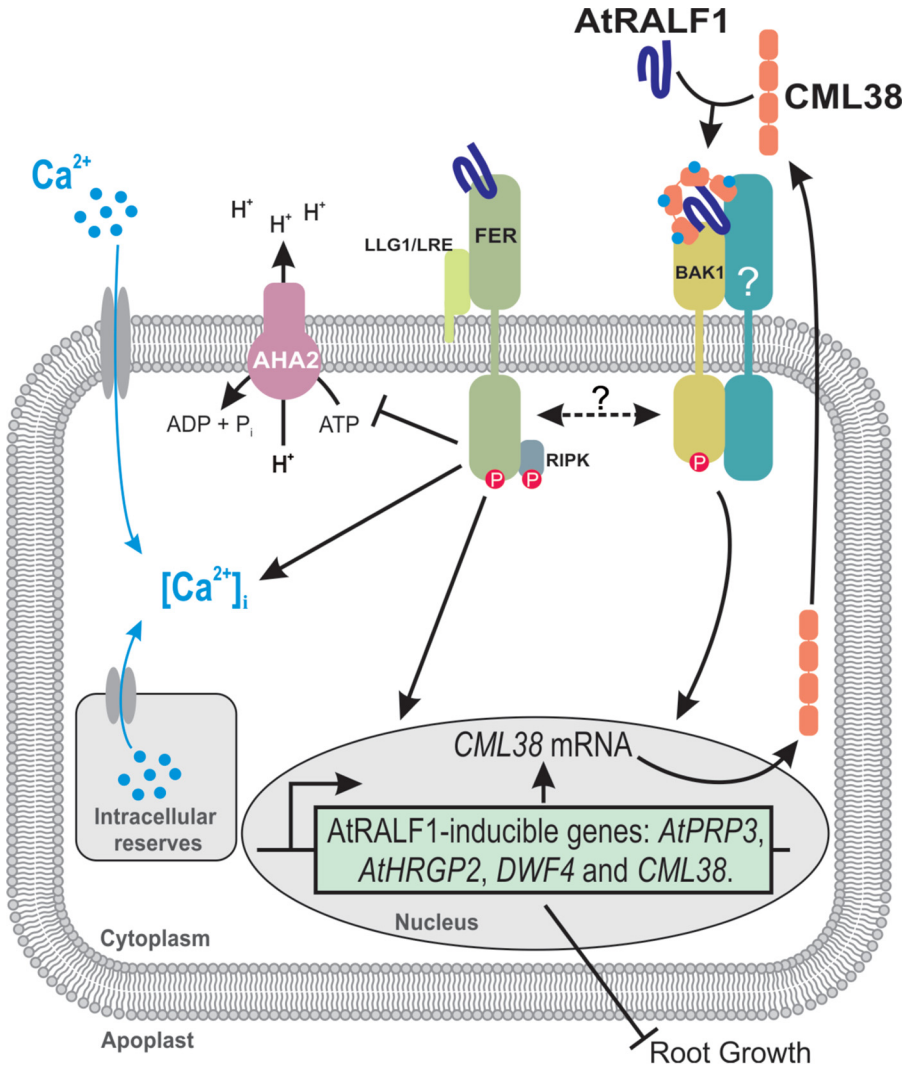

Figure 7. Proposed model for the involvement of CML38 in AtRALF1 recognition. In the plasma membrane, FER is complexed with LRE-like GPI-AP1 (LLG1)/LORELEI (LRE) protein and, upon AtRALF1 binding, recruits the receptor-like cytoplasmic kinase RIPK and inactivates the H^+-ATPase AHA2. Parallel to these events, the secreted protein CML38 binds to the AtRALF1 peptide and then to another receptor complex, probably involving BAK1 and another yet unknown plasma membrane receptor. Upon binding to the receptor, CML38-AtRALF1 up-regulates the expression of AtRALF1-inducible genes. The expression of these genes ultimately leads to root inhibition. In contrast to the AtRALF1 receptor FER, the CML38-AtRALF1 complex does not interfere with the plasma membrane H^+-ATPase AHA2. Both sets of receptors may cooperate in the observed root inhibition effect (*question marks*). *Solid lines* depict proven actions, and *intersecting lines* indicate putative actions. For more details, see "Discussion."

CML38 antibody. Additionally, AtRALF1-inducible genes would be repressed by CML38. In this case, such genes would also be induced in *cml38* genotypes. Interestingly, all previous information regarding RALF connects the inhibition of root growth with the alkalinization of the extracellular medium. When AtRALF1 binds to the plasma membrane, the H^+-ATPase AHA2 is phosphorylated and inhibited; this inhibition causes the alkalinization of the apoplast (4). The lack of an alkalinization effect in response to the addition of the CML38 protein (Fig. S11*A*) or the sequestration of the available protein by the antibody specific for CML38 (Fig. S11*B*) suggests that alkalinization and the inhibition of root growth may be dissociated. The sequestration of active CaMs that results from exposure to anti-CaM antibodies has been used to block the enhancer effect of CaMs on *Arabidopsis* cell suspension proliferation and pollen tube growth (31, 55). Recently, a role for RALFs as modulators of immune response has been proposed, and it has been suggested that their new function is independent of alkalinization activity (56).

The suggested dissociation of AtRALF1 biological activities motivated us to update our model for AtRALF1 recognition (Fig. 7). In this model, AtRALF1 has two different receptors on the plasma membrane. One receptor, FER, forms a complex with LRE-like GPI-AP1 (LLG1)/LORELEI (LRE) in the cell membrane and, when bound to AtRALF1, recruits the receptor-like cytoplasmic kinase RIPK and inactivates AHA2, leading to an increase in cytoplasmic Ca^{2+} (4, 13, 14, 15). We have recently identified the membrane protein BRI1-associated receptor kinase 1 (BAK1) as an AtRALF1 co-receptor (57). According to our model, upon AtRALF1 binding to FER, the H^+ flux is inhibited, leading to a transient alkalinization of the apoplast, causing the dissociation of BAK1 from the BRI1-BL-BAK1 complex (not depicted in the model) (57). Herein, we are proposing that AtRALF1 binds to apoplastic CML38 and then

to BAK1, recruiting or mediating the interaction with another yet unidentified receptor. The newly formed complex would then convey the message to inhibit root growth. There are data to support the existence of more than one RALF receptor. In tomato, tobacco, and alfalfa cell suspension cultures, incubation with a ^{125}I-azido-RALF resulted in labeled 120- and 25-kDa cell surface proteins (16). A biochemical characterization of the biological activities of nine AtRALFs also suggests the existence of multiple RALF receptors (10). In the FER mutant *fer4*, ~40% of ^{125}I-AtRALF1-specific binding was lost; insensitivity to AtRALF1-mediated root inhibition was specific but not complete in this mutant (4). Binding studies using acriAtRALF1 and *bak1* and *fer4* mutants demonstrated the existence of an apoplastic factor and more than two membrane receptor proteins (57). Taken together, these observations suggest that FER may depend on an association with other membrane proteins to regulate root inhibition. Our model proposes that CML38 is involved solely with this second, still unidentified, AtRALF1 receptor complex that probably involves BAK1. As *cml38* mutants have a normal alkalinization response, CML38 would not directly interact with FER. Our model is supported by the absolute requirement of CML38 for the root inhibitory effect of AtRALF1 and the normal alkalinization response shown by *cml38* mutants. Acridinium-labeled AtRALF1 specifically binds to intact roots of wildtype seedlings (Fig. 6). The proportion of the total binding that was AtRALF1-specific, as measured using acriAtRALF1, was similar to the specific binding measured with iodinated AtRALF1 in a previous study: 64% for acriAtRALF1 and ~50% in a *fer4* mutant (4). The proportion of the specific binding that depends on CML38 was also similar between our findings and those of the previous study, and this proportion did not overlap with the proportion that depends on FER, with an average of 46.5% for both *cml38* mutants in our study and 40% for the *fer4* mutant in the previous study (Fig. 6) (4). These results support the co-existence of two receptors, one dependent on CML38 and another dependent on FER. The acriAtRALF1 binding experiments show that CML38 is involved in the root inhibition effect of AtRALF1 and is essential for the binding of the AtRALF1 peptide to its receptor. The recovery of >80% of acriAtRALF1 binding in both *cml38* mutants when exogenous CML38 is supplied demonstrates the importance of CML38 in AtRALF1 binding.

Experimental procedures

Plant materials and growth conditions

The T-DNA insertion mutants *cml38-1* (SALK_066538), *cml38-2* (SALK_001571), and *cml39* (SALK_078400) were acquired from the ABRC (58). Plants overexpressing AtRALF1 were generated previously (10). Transgenic *Arabidopsis* plants were produced as described (59). The primers used for genotyping and semiquantitative RT-PCR are shown (Table S1). *Arabidopsis thaliana* (Col-0) seeds were surface-sterilized, stratified for 72 h at 4 °C, and then germinated on soil or in plates containing half-strength MS medium without sucrose and vitamins (pH 5.8) with or without Phytagel™ (Sigma-Aldrich). Plants on soil were grown in a Conviron growth chamber (16-h light, 150 μmol m^{-2} s^{-1}, and 8-h dark) at 22 ± 2 °C. The plates were kept in a growth room under the same light conditions. Wildtype *N. benthamiana* plants for agroinfiltration experiments were grown on soil under 14-h light and 10-h dark at 22 ± 2 °C.

Two-hybrid system in yeast

The full-length coding sequence of the AtRALF1 precursor (locus At1g02900) was fused to the GAL4 DNA-binding domain using the NdeI/BamHI sites in the pGBKT7 (Clontech) bait expression vector. The construct was then transformed into the yeast strain AH109 as described previously (60). The resultant yeast cells were transformed with a λACT two-hybrid cDNA library (CD4-10 from ABRC). Yeast two-hybrid screening was performed using the Matchmaker GAL4 Two-Hybrid System 3 (Clontech). Yeast transformants were screened on a synthetic complete medium lacking leucine, tryptophan, and histidine. Plasmid DNA was recovered from positive yeast colonies, and the *E. coli* strain DH5α (TOP10, Life Technologies, Inc.) was transformed with these plasmids. Plasmid DNA was isolated from *E. coli* cultures for sequencing. The full-length coding regions of *CML37* (At5g42380), *CML38* (At1g76650), *CML39* (At1g76640), *AtRALF34* (At5g67070), and *AtRALF1*, as well as *AtRALF1* deletions, were amplified from *Arabidopsis* genomic DNA or cDNA and cloned into pGBKT7 or pGADT7 vectors, as indicated, for further testing. The transformed cells were selected on synthetic complete medium lacking leucine, tryptophan, and histidine. A list of all primers used is available (Table S1).

Recombinant proteins and the in vitro pulldown assay

AtRALF1, CML38, and CML39 coding regions were amplified by conventional PCR using specific primers (Table S1). The amplified AtRALF1 coding region was cloned into the pET28b vector at the NdeI/HindIII restriction sites. The amplified fragments coding for the truncated and inactive peptide AtRALF1(9–49), CML38, and CML39 were cloned into the pENTR D-TOPO (Life Technologies) vector and transferred to the pDEST17 (Life Technologies) vector by recombination. All of the peptides were fused to a histidine tag at their N termini. The vectors were then introduced into the *E. coli* strain Rosetta DE3. The recombinant proteins AtRALF1, AtRALF1(9–49), CML38, and CML39 were produced, purified, and analyzed as described (10). After affinity purification, the recombinant peptides AtRALF1 and AtRALF1(9–49) were dialyzed against 1% (v/v) formic acid (5 × 4 liters in 4 days at 4 °C) and later freeze-dried. CML38 and CML39 were suspended in phosphate-buffered saline buffer. GST fusion proteins were purified and bound to glutathione-agarose beads (Thermo Scientific) as described (61, 62). Purified GST-tagged fusion proteins were lyophilized and suspended in phosphate-buffered saline buffer. Purified proteins were combined in a total volume of 200 μl of interaction buffer (8 mM NaH_2PO_4, 2.7 mM KH_2PO_4, 100 mM NaCl, 2.7 mM KCl, 1 mM phenylmethylsulfonyl fluoride, 0.05% (v/v) Tween supplemented or not with 1 mM $CaCl_2$ and 10 mM EGTA) at pH 6.5 or 7.5 and incubated overnight at 4 °C. This solution was incubated with glutathione-agarose beads (Thermo Scientific) for 30 min at 4 °C. The beads were washed five times with interaction buffer, and proteins were eluted in

40 μl of cold elution buffer (50 mM Tris-HCl, pH 8.0, 10 mM reduced glutathione). The eluted proteins were analyzed by protein blotting. Anti-AtRALF1 (1:2000) and anti-CML38 (1:5000) rabbit antibodies were produced by CelulaB, UFRGS (Brazil). Blots were visualized using an AP-conjugated anti-rabbit IgG (Bio-Rad; 1:30,000) and Lumi-Phos WB (Pierce) or horseradish peroxidase–conjugated anti-rabbit IgG (Bio-Rad; 1:30,000) and SuperSignal West Femto (Thermo Fisher Scientific). All experiments were repeated at least three times (independent biological replicates).

Isothermal titration calorimetry

ITC experiments were performed using a VP isothermal titration calorimeter with a 1.4-ml standard cell and a 293-μl titration syringe. Proteins were dissolved in 15 mM HEPES, pH 6.8, ITC buffer before all titrations. Molar protein concentrations for CML38 and AtRALF1 were calculated using their molecular masses of 27,551 and 7,631 Da, respectively, and 8 mg of each recombinant protein (HPLC-purified). Experiments were performed at 25 °C. The concentrations for the complex titrations were 0.3 mM ligand (AtRALF1) in the syringe and 0.03 mM protein (CML38) and 1 mM calcium chloride or 1 mM EDTA mixture in the cell at time intervals of 300 s (28 injections of volume 10 μl) to ensure that the titration peak returned to the baseline. ITC data were corrected for the heat of dilution by subtracting the mixing enthalpies for titrant solution injections into protein free ITC buffer. Data were analyzed using the Origin software as provided by the manufacturer. Independent experiments were repeated at least twice with similar results.

Subcellular localization

All recombinant plasmids were introduced into *Agrobacterium tumefaciens* (GV3101) and used for transient expression assays in *N. benthamiana* leaves. Transient expression assays were performed as described previously (63). The viral RNA silencing suppressor p19 protein was co-infiltrated with all constructions to ensure the appropriate level of transient expression. For plasmolysis experiments, leaves of transgenic *N. benthamiana* were incubated for 30 min in a 0.8 M mannitol solution. Epidermal cells of *N. benthamiana* leaves were analyzed 3–7 days post-infiltration for subcellular localization. Analyses were performed using an inverted Olympus FluoView 1000 confocal laser-scanning microscope. GFP and FM4-64 were excited at 488 and 515 nm, respectively, with an argon ion laser. Fluorescent emissions recovered in the 505–530-nm interval corresponded to GFP; emissions in the 630–650-nm interval correspond to FM4-64. All transient expression assays were repeated at least three times with independent biological replicates, and consistent results were obtained. BFA (30 μM) was infiltrated in transiently transformed *N. benthamiana* leaves for 2 h. Roots were treated with BFA for 45 min. BFA bodies were stained with 2 μM FM4-64 dye for 15 min. Stock solutions were made using DMSO (BFA, 5 mM) and water (FM4-64, 2 mM).

Plant transformation

The *AtRALF1* sequence cloned into the pENTR/D-TOPO vector was transferred by recombination into the destination vector pK7FWG2. The *PROAtRALF1:AtRALF1:GFP:T35S* sequence (2556 bp) was amplified and cloned into pENTR/D-TOPO. The fragment was transferred by recombination into the destination vector pKGWFS7 (64). The *CML38* sequence cloned into the pENTR/D-TOPO vector was transferred into pK7WG2. To generate the *PROCML38:CML38:GFP* vector, the *CML38* gene and a 1438-bp genomic region upstream were amplified using specific primers (Table S1). The *PROCML38:CML38* fragment (1973 bp) was inserted into the pENTR/D-TOPO vector and transferred by recombination to the pK7FWG2 vector. The mRFP-KDEL clone was generated using the ST-mRFP vector (65) introducing the -KDEL sequence at the C terminus by conventional PCR using specific primers (Table S1). The *A. tumefaciens* (GV3101) was used for the stable transformation of *Arabidopsis* using the floral dip method (66). Transgene expression was confirmed using semiquantitative RT-PCR (Table S1). Third generation (T3) transgenic lines were used.

Root growth, hypocotyl elongation, and alkalinization assays

Aliquots of half-strength MS liquid medium (1 ml) containing seeds were distributed into 24-well plates. Unless stated otherwise, 2 μM AtRALF1 and 2 μM CML38 or CML39 were added after 48 h. Alternatively, seeds were germinated in vertical plates with half-strength MS medium containing 9 g liter^{-1} Phytagel™. The plates were incubated in the growth room for the times indicated. The seedlings were then transferred to new plates with the same medium containing AtRALF1 or a peptide-free medium. Root length was measured 8 days after treatment or as indicated. Quantitative data were obtained as described (59). A lithium sensitivity assay was performed as described (4). The plates were exposed to light for 1 h and then incubated for 24 h in the dark for the hypocotyl elongation assay. Hypocotyl growth was evaluated 2 days after treatment. Alkalinization assays were performed as described (10). All experiments were repeated at least three times using independent biological replicates.

Binding assay using acridinium-labeled AtRALF1

Acridinium NHS esters were conjugated to the terminal amino group of the AtRALF1 peptide according to the manufacturer's instructions (Cayman Chemical). The acriAtRALF1 was separated from the unlabeled peptide and quantified by HPLC. Five-day-old seedlings were incubated with acriAtRALF1 and different concentrations of AtRALF1, CML38, or CML39 for 15 min at 4 °C on a shaker. After incubation, the seedlings were washed three times with half-strength MS medium. Five seedlings or roots were used per treatment. The resulting luminescence emissions from the acridinium in whole seedlings or roots were measured using a microplate reader (Biotec ELx 800) at 2 s after injecting 50 μl of a solution containing 20 mM H_2O_2 in 0.1 M NaOH. The cytoplasmic Ca^{2+} assay was performed as described previously (22). The experiments were repeated at least three times using independent biological replicates. Duplicates were used for each concentration or treatment. Data shown are from one representative experiment.

Author contributions—W.F.C., K.D., and C.S.F. performed Y2H and contributed for CML38 subcellular localization experiments. W.F.C. performed pulldown experiments and analyzed *PRO35S:CML38* plants. W.F.C, K.D., and P.H.O.C performed CML38 mutant analysis. K.D. and P.H.O.C. performed acridinium-labeled AtRALF1 experiments. J.C.G.-A. and W.F.C. obtained and analyzed all hybrids and performed protein blot experiments. J.C.G.-A. and L.A.N.C. performed all confocal microscopy work. A.L.S performed ITC assays. P.H.O.C. and A.M.C. produced recombinant proteins and performed alkalinization assays. T.B. and W.F.C. performed gene expression experiments. M.C.S.-F. contributed ideas and data interpretation. D.S.M. designed the research, compiled the data, and coordinated the writing of the manuscript. All authors reviewed the results and approved the final version of the manuscript.

Acknowledgments—We thank A.F.C. Amaral for technical assistance with plants and cells; Dr. L.E.P. Peres and C.R.F. Figueiredo for technical assistance with the luminescence assay; and Dr. C.A. Montanari, Dr. A. Leitão, and F. Rosini for technical assistance with the ITC assay.

References

1. Pearce, G., Moura, D. S., Stratmann, J., and Ryan, C. A. (2001) RALF, a 5-kDa ubiquitous polypeptide in plants, arrests root growth and development. *Proc. Natl. Acad. Sci. U.S.A.* **98,** 12843–12847 CrossRef Medline
2. Masachis, S., Segorbe, D., Turrà, D., Leon-Ruiz, M., Fürst, U., El Ghalid, M., Leonard, G., López-Berges, M. S., Richards, T. A., Felix, G., and Di Pietro, A. (2016) A fungal pathogen secretes plant alkalinizing peptides to increase infection. *Nat. Microbiol.* **1,** 16043 CrossRef Medline
3. Mingossi, F. B., Matos, J. L., Rizzato, A. P., Medeiros, A. H., Falco, M. C., Silva-Filho, M. C., and Moura, D. S. (2010) SacRALF1, a peptide signal from the grass sugarcane (*Saccharum* spp.), is potentially involved in the regulation of tissue expansion. *Plant Mol. Biol.* **73,** 271–281 CrossRef Medline
4. Haruta, M., Sabat, G., Stecker, K., Minkoff, B. B., and Sussman, M. R. (2014) A peptide hormone and its receptor protein kinase regulate plant cell expansion. *Science* **343,** 408–411 CrossRef Medline
5. Murphy, E., and De Smet, I. (2014) Understanding the RALF family: a tale of many species. *Trends Plant Sci.* **19,** 664–671 CrossRef Medline
6. Escobar, N. M., Haupt, S., Thow, G., Boevink, P., Chapman, S., and Oparka, K. (2003) High-throughput viral expression of cDNA-green fluorescent protein fusions reveals novel subcellular addresses and identifies unique proteins that interact with plasmodesmata. *Plant Cell* **15,** 1507–1523 CrossRef Medline
7. Bedinger, P. A., Pearce, G., and Covey, P. A. (2010) RALFs: Peptide regulators of plant growth. *Plant Signal Behav.* **5,** 1342–1346 CrossRef Medline
8. Cao, J., and Shi, F. (2012) Evolution of the *RALF* gene family in plants: gene duplication and selection patterns. *Evol. Bioinform. Online* **8,** 271–292 Medline
9. Lamesch, P., Berardini, T. Z., Swarbreck, D., Wilks, C., Sasidharan, R., Muller, R., Dreher, K., Alexander, D. L., Garcia-Hernandez, M., Karthikeyan, A. S., Lee, C. H., Nelson, W. D., Ploetz, L., Singh, S., Wensel, A., and Huala, E. (2011) The Arabidopsis Information Resource (TAIR): improved gene annotation and new tools. *Nucleic Acids Res.* **40,** D1202–D1210 CrossRef Medline
10. Morato do Canto, A., Ceciliato, P. H. O., Ribeiro, B., Ortiz-Morea, F. A., Franco Garcia, A. A., Silva-Filho, M. C., and Moura, D. S. (2014) Biological activity of nine recombinant AtRALF peptides: implications for their perception and function in *Arabidopsis*. *Plant Physiol. Biochem.* **75,** 45–54 CrossRef Medline
11. Matos, J. L., Fiori, C. S., Silva-Filho, M. C., and Moura, D. S. (2008) A conserved dibasic site is essential for correct processing of the peptide hormone AtRALF1 in *Arabidopsis thaliana*. *FEBS Lett.* **582,** 3343–3347 CrossRef Medline
12. Srivastava, R., Liu, J. X., Guo, H., Yin, Y., and Howell, S. H. (2009) Regulation and processing of a plant peptide hormone, AtRALF23, in *Arabidopsis*. *Plant J.* **59,** 930–939 CrossRef Medline
13. Li, C., Yeh, F. L., Cheung, A. Y., Duan, Q., Kita, D., Liu, M. C., Maman, J., Luu, E. J., Wu, B. W., Gates, L., et al. (2015) Glycosylphosphatidylinositol-anchored proteins as chaperones and co-receptors for FERONIA receptor kinase signaling in *Arabidopsis*. *eLife* **4,** e06587 CrossRef Medline
14. Li, C., Wu, H. M., and Cheung, A. Y. (2016) FERONIA and her pals: functions and mechanisms. *Plant Physiol.* **171,** 2379–2392 Medline
15. Du, C., Li, X., Chen, J., Chen, W., Li, B., Li, C., Wang, L., Li, J., Zhao, X., Lin, J., Liu, X., Luan, S., and Yu, F. (2016) Receptor kinase complex transmits RALF peptide signal to inhibit root growth in *Arabidopsis*. *Proc. Natl. Acad. Sci. U.S.A.* **113,** E8326–E8334 CrossRef Medline
16. Scheer, J. M., Pearce, G., and Ryan, C. A. (2005) *Le*RALF, a plant peptide that regulates root growth and development, specifically binds to 25 and 120 kDa cell surface membrane proteins of *Lycopersicon peruvianum*. *Planta* **221,** 667–674 CrossRef Medline
17. Atkinson, N. J., Lilley, C. J., and Urwin, P. E. (2013) Identification of genes involved in the response of *Arabidopsis* to simultaneous biotic and abiotic stresses. *Plant Physiol.* **162,** 2028–2041 CrossRef Medline
18. Wu, J., Kurten, E. L., Monshausen, G., Hummel, G. M., Gilroy, S., and Baldwin, I. T. (2007) NaRALF, a peptide signal essential for the regulation of root hair tip apoplastic pH in *Nicotiana attenuata*, is required for root hair development and plant growth in native soils. *Plant J.* **52,** 877–890 CrossRef Medline
19. Bergonci, T., Ribeiro, B., Ceciliato, P. H. O., Guerrero-Abad, J. C., Silva-Filho, M. C., and Moura, D. S. (2014) *Arabidopsis thaliana* RALF1 opposes brassinosteroid effects on root cell elongation and lateral root formation. *J. Exp. Bot.* **65,** 2219–2230 CrossRef Medline
20. Hepler, P. K. (2005) Calcium: a central regulator of plant growth and development. *Plant Cell* **17,** 2142–2155 CrossRef Medline
21. Kudla, J., Batistic, O., and Hashimoto, K. (2010) Calcium signals: the lead currency of plant information processing. *Plant Cell* **22,** 541–563 CrossRef Medline
22. Haruta, M., Monshausen, G., Gilroy, S., and Sussman, M. R. (2008) A cytoplasmic Ca^{2+} functional assay for identifying and purifying endogenous cell signaling peptides in *Arabidopsis* seedlings: identification of AtRALF1 peptide. *Biochemistry* **47,** 6311–6321 CrossRef Medline
23. McCormack, E., and Braam, J. (2003) Calmodulins and related potential calcium sensors of *Arabidopsis*. *New Phytol.* **159,** 585–598 CrossRef
24. Clapham, D. E. (2007) Calcium signaling. *Cell* **131,** 1047–1058 CrossRef Medline
25. McCormack, E., Tsai, Y. C., and Braam, J. (2005) Handling calcium signaling: *Arabidopsis* CaMs and CMLs. *Trends Plant Sci.* **10,** 383–389 CrossRef Medline
26. Chin, D., and Means, A. R. (2000) Calmodulin: a prototypical calcium sensor. *Trends Cell Biol.* **10,** 322–328 CrossRef Medline
27. Snedden, W. A., and Fromm, H. (2001) Calmodulin as a versatile calcium signal transducer in plants. *New Phytol.* **151,** 35–66 CrossRef
28. Popescu, S. C., Popescu, G. V., Bachan, S., Zhang, Z., Seay, M., Gerstein, M., Snyder, M., and Dinesh-Kumar, S. P. (2007) Differential binding of calmodulin-related proteins to their targets revealed through high-density *Arabidopsis* protein microarrays. *Proc. Natl. Acad. Sci. U.S.A.* **104,** 4730–4735 CrossRef Medline
29. Bürstenbinder, K., Savchenko, T., Müller, J., Adamson, A. W., Stamm, G., Kwong, R., Zipp, B. J., Dinesh, D. C., and Abel, S. (2013) *Arabidopsis* calmodulin-binding protein IQ67-domain 1 localizes to microtubules and interacts with kinesin light chain-related protein-1. *J. Biol. Chem.* **288,** 1871–1882 CrossRef Medline
30. Bürstenbinder, K., Möller, B., Plötner, R., Stamm, G., Hause, G., Mitra, D., and Abel, S. (2017) The IQD family of calmodulin-binding proteins links calcium signaling to microtubules, membrane subdomains, and the nucleus. *Plant Physiol.* **173,** 1692–1708 CrossRef Medline
31. Cui, S., Guo, X., Chang, F., Cui, Y., Ma, L., Sun, Y., and Sun, D. (2005) Apoplastic calmodulin receptor-like binding proteins in suspension-cul-

tured cells of *Arabidopsis thaliana*. *J. Biol. Chem.* **280,** 31420–31427 CrossRef Medline
32. Wang, Q., Chen, B., Liu, P., Zheng, M., Wang, Y., Cui, S., Sun, D., Fang, X., Liu, C. M., Lucas, W. J., and Lin, J. (2009) Calmodulin binds to extracellular sites on the plasma membrane of plant cells and elicits a rise in intracellular calcium concentration. *J. Biol. Chem.* **284,** 12000–12007 CrossRef Medline
33. Day, I. S., Reddy, V. S., Shad Ali, G., and Reddy, A. S. (2002) Analysis of EF-hand-containing proteins in *Arabidopsis*. *Genome Biol.* **3,** RESEARCH0056.1–0056.24 Medline
34. Scholz, S. S., Vadassery, J., Heyer, M., Reichelt, M., Bender, K. W., Snedden, W. A., Boland, W., and Mithöfer, A. (2014) Mutation of the *Arabidopsis* calmodulin-like protein CML37 deregulates the jasmonate pathway and enhances susceptibility to herbivory. *Mol. Plant* **7,** 1712–1726 CrossRef Medline
35. Vanderbeld, B., and Snedden, W. A. (2007) Developmental and stimulus-induced expression patterns of *Arabidopsis* calmodulin-like genes CML37, CML38 and CML39. *Plant Mol. Biol.* **64,** 683–697 CrossRef Medline
36. Lokdarshi, A., Conner, W. C., McClintock, C., Li, T., and Roberts, D. M. (2016) *Arabidopsis* CML38, a calcium sensor that localizes to ribonucleoprotein complexes under hypoxia stress. *Plant Physiol.* **170,** 1046–1059 CrossRef Medline
37. Bender, K. W., Rosenbaum, D. M., Vanderbeld, B., Ubaid, M., and Snedden, W. A. (2013) The *Arabidopsis* calmodulin-like protein, CML39, functions during early seedling establishment. *Plant J.* **76,** 634–647 CrossRef Medline
38. Covey, P. A., Subbaiah, C. C., Parsons, R. L., Pearce, G., Lay, F. T., Anderson, M. A., Ryan, C. A., and Bedinger, P. A. (2010) A pollen-specific RALF from tomato that regulates pollen tube elongation. *Plant Physiol.* **153,** 703–715 CrossRef Medline
39. Chen, J., Yu, F., Liu, Y., Du, C., Li, X., Zhu, S., Wang, X., Lan, W., Rodriguez, P. L., Liu, X., Li, D., Chen, L., and Luan, S. (2016) FERONIA interacts with ABI2-type phosphatases to facilitate signaling cross-talk between abscisic acid and RALF peptide in *Arabidopsis*. *Proc. Natl. Acad. Sci. U.S.A.* **113,** E5519–E5527 CrossRef Medline
40. Pierce, M. M., Raman, C. S., and Nall, B. T. (1999) Isothermal titration calorimetry of protein–protein interactions. *Methods* **19,** 213–221 CrossRef Medline
41. Bolte, S., and Cordelières, F. P. (2006) A guided tour into subcellular colocalization analysis in light microscopy. *J. Microsc.* **224,** 213–232 CrossRef Medline
42. Geldner, N., Hyman, D. L., Wang, X., Schumacher, K., and Chory, J. (2007) Endosomal signaling of plant steroid receptor kinase BRI1. *Gene Dev.* ***21,*** 1598–1602 CrossRef Medline
43. Bendtsen, J. D., Jensen, L. J., Blom, N., Von Heijne, G., and Brunak, S. (2004) Feature-based prediction of non-classical and leaderless protein secretion. *Protein Eng. Des. Sel.* **17,** 349–356 CrossRef Medline
44. Butenko, M. A., Wildhagen, M., Albert, M., Jehle, A., Kalbacher, H., Aalen, R. B., and Felix, G. (2014) Tools and strategies to match peptide-ligand receptor pairs. *Plant Cell* **26,** 1838–1847 CrossRef Medline
45. Bender, K. W., and Snedden, W. A. (2013) Calmodulin-related proteins step out from the shadow of their namesake. *Plant Physiol.* **163,** 486–495 CrossRef Medline
46. Grignon, C., and Sentenac, H. (1991) pH and ionic conditions in the apoplast. *Annu. Rev. Plant Physiol. Plant Mol. Biol* **42,** 103–128 CrossRef
47. Bibikova, T. N., Jacob, T., Dahse, I., and Gilroy, S. (1998) Localized changes in apoplastic and cytoplasmic pH are associated with root hair development in *Arabidopsis thaliana*. *Development* **125,** 2925–2934 Medline
48. Yamaguchi, T., Aharon, G. S., Sottosanto, J. B., and Blumwald, E. (2005) Vacuolar Na^+/H^+ antiporter cation selectivity is regulated by calmodulin from within the vacuole in a Ca^{2+}- and pH-dependent manner. *Proc. Natl. Acad. Sci. U.S.A.* **102,** 16107–16112 CrossRef Medline
49. Biro, R. L., Daye, S., Serlin, B. S., Terry, M. E., Datta, N., Sopory, S. K., and Roux, S. J. (1984) Characterization of oat calmodulin and radioimmunoassay of its subcellular distribution. *Plant Physiol.* **75,** 382–386 CrossRef Medline
50. Sun, D. Y., Li, H. B., and Cheng, G. (1994) Extracellular calmodulin accelerates the proliferation of suspension-cultured cells of *Angelica dahurica*. *Plant Sci.* **99,** 1–8 CrossRef
51. Sun, D. Y., Bian, Y. Q., Zhao, B. H., and Zhao, L. Y. (1995) The effects of extracellular calmodulin on cell wall regeneration of protoplasts and cell division. *Plant Cell Physiol.* **36,** 133–138
52. Ma, L., and Sun, D. (1997) The effects of extracellular calmodulin on initiation of *Hippeastrum rutilum* pollen germination and tube growth. *Planta* **202,** 336–340 CrossRef
53. Stinemetz, C. L., Hasenstein, K. H., Young, L. M., and Evans, M. L. (1992) Effect of calmodulin antagonists on the growth and graviresponsiveness of primary roots of maize. *Plant Growth Regul.* **11,** 419–427 CrossRef Medline
54. Zhao, Q., Zhang, C., Jia, Z., Huang, Y., Li, H., and Song, S. (2014) Involvement of calmodulin in regulation of primary root elongation by *N*-3-oxo-hexanoyl homoserine lactone in *Arabidopsis thaliana*. *Front. Plant Sci.* **5,** 807 Medline
55. Ma, L., Xu, X., Cui, S., and Sun, D. (1999) The presence of a heterotrimeric G protein and its role in signal transduction of extracellular calmodulin in pollen germination and tube growth. *Plant Cell* **11,** 1351–1364 CrossRef Medline
56. Stegmann, M., Monaghan, J., Smakowska-Luzan, E., Rovenich, H., Lehner, A., Holton, N., Belkhadir, Y., and Zipfel, C. (2017) The receptor kinase FER is a RALF-regulated scaffold controlling plant immune signaling. *Science* **355,** 287–289 CrossRef Medline
57. Dressano, K., Ceciliato, P. H. O., Silva, A. L., Guerrero-Abad, J. C., Bergonci, T., Ortiz-Morea, F. A., Bürger, M., Silva-Filho, M. C., and Moura, D. S. (2017) BAK1 is involved in AtRALF1-induced inhibition of root cell expansion. *PLoS Genet.* **13,** e1007053 CrossRef Medline
58. Alonso, J. M., Stepanova, A. N., Leisse, T. J., Kim, C. J., Chen, H., Shinn, P., Stevenson, D. K., Zimmerman, J., Barajas, P., Cheuk, R., Gadrinab, C., Heller, C., Jeske, A., Koesema, E., Meyers, C. C., *et al.* (2003) Genome-wide insertional mutagenesis of *Arabidopsis thaliana*. *Science* **301,** 653–657 CrossRef Medline
59. Weigel, D., and Glazebrook, J. (2002) *Arabidopsis: A Laboratory Manual*, 1st Ed., Cold Spring Harbor Laboratory, Cold Spring Harbor, NY
60. Gietz, R. D., and Woods, R. A. (2006) Yeast transformation by the LiAc/SS carrier DNA/PEG method. *Methods Mol. Biol.* **313,** 107–120 Medline
61. Frangioni, J. V., and Neel, B. G. (1993) Solubilization and purification of enzymatically active glutathione *S*-transferase (pGEX) fusion proteins. *Anal. Biochem.* **210,** 179–187 CrossRef Medline
62. Arazi, T., Baum, G., Snedden, W. A., Shelp, B. J., and Fromm, H. (1995) Molecular and biochemical analysis of calmodulin interactions with the calmodulin-binding domain of plant glutamate decarboxylase. *Plant Physiol.* **108,** 551–561 CrossRef Medline
63. Sparkes, I. A., Runions, J., Kearns, A., and Hawes, C. (2006) Rapid, transient expression of fluorescent fusion proteins in tobacco plants and generation of stably transformed plants. *Nat. Protoc.* **1,** 2019–2025 CrossRef Medline
64. Karimi, M., Inzé, D., and Depicker, A. (2002) GATEWAY™ vectors for *Agrobacterium*-mediated plant transformation. *Trends Plant Sci.* **7,** 193–195 CrossRef Medline
65. Osterrieder, A., Hummel, E., Carvalho, C. M., and Hawes, C. (2010) Golgi membrane dynamics after induction of a dominant-negative mutant Sar1 GTPase in tobacco. *J. Exp. Bot.* **61,** 405–422 CrossRef Medline
66. Clough, S. J., and Bent, A. F. (1998) Floral dip: a simplified method for *Agrobacterium*-mediated transformation of *Arabidopsis thaliana*. *Plant J.* **16,** 735–743 CrossRef Medline